https://doi.org/10.5607/en23020
Exp Neurobiol. 2023 Aug;32(4):271-284.
pISSN 1226-2560 • eISSN 2093-8144

Original Article

Experimental Neurobiology

Bias in Prestimulus Motor Cortical Activity Determines Decision-making Error in Rodents

Soyoung Chae, Duho Sihn and Sung-Phil Kim*
Department of Biomedical Engineering, Ulsan National Institute of Science and Technology, Ulsan 44919, Korea

Decision-making is a complex process that involves the integration and interpretation of sensory information to guide actions. The rodent motor cortex, which is generally involved in motor planning and execution, also plays a critical role in decision-making processes. In perceptual delayed-response tasks, the rodent motor cortex can represent sensory cues, as well as the decision of where to move. However, it remains unclear whether erroneous decisions arise from incorrect encoding of sensory information or improper utilization of the collected sensory information in the motor cortex. In this study, we analyzed the rodent anterior lateral motor cortex (ALM) while the mice performed perceptual delayed-response tasks. We divided population activities into sensory and choice signals to separately examine the encoding and utilization of sensory information. We found that the encoding of sensory information in the error trials was similar to that in the hit trials, whereas choice signals evolved differently between the error and hit trials. In error trials, choice signals displayed an offset in the opposite direction of instructed licking even before stimulus presentation, and this tendency gradually increased after stimulus onset, leading to incorrect licking. These findings suggest that decision errors are caused by biases in choice-related activities rather than by incorrect sensory encoding. Our study elaborates on the understanding of decision-making processes by providing neural substrates for erroneous decisions.

Key words: Decision making, Motor cortex, Mice

INTRODUCTION

Animals make accurate decisions by effectively gathering and processing sensory evidence from their environment. Sensory information generated from multiple sensory brain regions is transmitted to other brain regions involved in decision-making [1]. For example, the anterior lateral motor cortex (ALM) is involved in decision-making through the deliberation of appropriate actions based on sensory evidence [2-8]. Perturbations of sensory channels from the sensory cortex or thalamus to the ALM disrupt the encoding of sensory information in the ALM, resulting in incorrect decisions [9, 10]. Additionally, perturbing the ALM during the early phase of decision-making can lead to erroneous decisions [6, 7]. These findings indicate that multiple stages of decision-making must remain intact to make an accurate decision.

In the absence of neural circuit modulation, even skillfully trained animals occasionally make erroneous decisions. Such decision errors can occur when the probabilistic coding of sensory information in neural populations is disrupted or misinterpreted [11]. For example, in the tactile delayed-response task where mice licked to the right or left according to a tactile cue, which involved the stimulation of the touch location on their whiskers a few seconds before the response, the majority of ALM neurons revealed a selective firing activity tuned to touch location or lick direction, known as selectivity [6, 9, 12]. The selectivity of ALM neurons is systematically altered during error trials [13]. However, it remains unclear whether altered selectivity and consequent erroneous decisions stem from incorrect sensory information encoding or improper use of collected sensory information throughout the decision-making process.

Submitted July 7, 2023, Revised August 23, 2023,
Accepted August 30, 2023

*To whom correspondence should be addressed.
TEL: 82-52-217-2727, FAX: 82-52-217-2708
e-mail: spkim@unist.ac.kr

To address this question, the present study aimed to analyze ALM activity in perceptual delayed-response tasks. In this task, mice received a sensory cue during the sample period, waited for a go cue during the delay period, and licked to the left or right during the response period. Specifically, we compared two different datasets, each involving a different sensory stimulus (tactile vs. auditory) during the sample period, to investigate whether neural substrates of decision-making errors were consistent across sensory modalities. We divided the ALM population activities into sensory and choice signals to examine the encoding and utilization of sensory information separately. Sensory signals, inferred from the population activities that differentiated stimuli during the sample period, maintained a certain level of distinction between different sensory stimuli in the error trials. Yet, the level of distinction in the error trials was less pronounced than that in the hit trials. In contrast, choice signals derived from population activities that discriminated between choices during the delay period increased in the direction of the instructed licking movement in the hit trials. However, in the error trials, the choice signals exhibited a prestimulus offset in a direction opposite to the instructed licking movement. Furthermore, after the error trial began, the choice signals showed a gradually increasing tendency in the direction opposite to the instructed licking movement, without bias correction. In conclusion, our findings suggest that errors in decision-making are not attributed to incorrect encoding of sensory information but involve the presence of biases in choice before gathering sensory information, which is not corrected by the collected sensory information.

MATERIALS AND METHODS

Behavioral task

This study analyzed two separate open datasets obtained from the following data-sharing websites: Collaborative Research in Computational Neuroscience (CRCNS.org) for the tactile delayed-response task [14] and FigShare for the auditory delayed-response task (https://doi.org/10.25378/janelia.7489253). Detailed descriptions of the data collection procedure can be found in the studies by Inagaki et al. and Li et al. [4-6]. Briefly, the mice were trained to learn the perceptual delayed-response task (Fig. 1A, B).

In the first dataset, 19 mice were trained to discriminate tactile stimuli in a tactile delayed-response task. At the beginning of this task, the pole touched an anterior or posterior whisker for 1.3 s (sample period, Fig. 1A). Following a temporal delay of 1.3 s (delay period, Fig. 1A), a non-selective auditory go cue was given, and the mice licked to the right or left based on the given tactile stimulus to receive a water reward (response period, Fig. 1A). In the second dataset, six mice were trained to discriminate auditory stimuli using an auditory delayed-response task. In this task, an auditory stimulus was presented at one of the two frequencies, 3 or 12 kHz, for 1.15 s. This was followed by a delay period of 2 s. The response period was the same as that of the first dataset (Fig. 1B).

In the first dataset, the mice were trained to discriminate between tactile stimuli in a tactile delayed-response task. At the beginning of this task, the pole touched an anterior or posterior whisker for 1.3 s (sample period, Fig. 1A). Following a temporal delay of 1.3 s (delay period, Fig. 1A), a non-selective auditory go cue was given, and the mice licked right or left based on the given tactile stimulus to receive a water reward (response period, Fig. 1A). In the second dataset, a different group of mice was trained to discriminate between auditory stimuli in an auditory delayed-response task. In this task, an auditory stimulus was presented at one of the two frequencies: 3 or 12 kHz, for 1.15 s. This was followed by a delay period of 2 s. The response period was the same as that of the first dataset (Fig. 1B).

Extracellular recording data analysis

Action potentials (spikes) were simultaneously recorded in the left ALM by using 32-channel NeuroNexus silicon probes (Part No. A4×8-5mm-100-200-177) for the tactile delayed-response task and 64-channel Janelia silicon probes for the auditory delayed-response task. Spike data were obtained from CRCNS.org for the tactile delayed-response task and from FigShare for the auditory delayed-response task. Extracellular traces were recorded from the left ALM and bandpass-filtered (300~6,000 Hz). Spike width was calculated as the trough-to-peak interval in the average spike waveform. Units with spike width narrower than 0.35 ms were classified as putative fast-spiking neurons, whereas those wider than 0.5 ms were defined as putative pyramidal neurons. In the tactile delayed-response task, 1,368 units were identified. Among them, 112 were putative fast-spiking neurons and 1,137 were putative pyramidal neurons. The remaining 109 units with intermediate spike widths were excluded from analysis. In the auditory delayed-response task, 755 units were identified, of which 74 were putative fast-spiking neurons and 667 were putative pyramidal neurons; the remaining 11 units with intermediate spike widths were excluded from the analysis.

Firing rates were computed with a 50 ms-sized squared bin at every 1 ms (98% overlap between successive bins). Baseline subtraction and magnitude normalization were then applied to the firing rates of single trials for each neuron. The baseline duration was determined as 0~550 ms before the stimulus was given. For magnitude normalization, we first averaged the firing rates of a neuron across every trial. We then calculated a vector length of the aver-

https://doi.org/10.5607/en23020

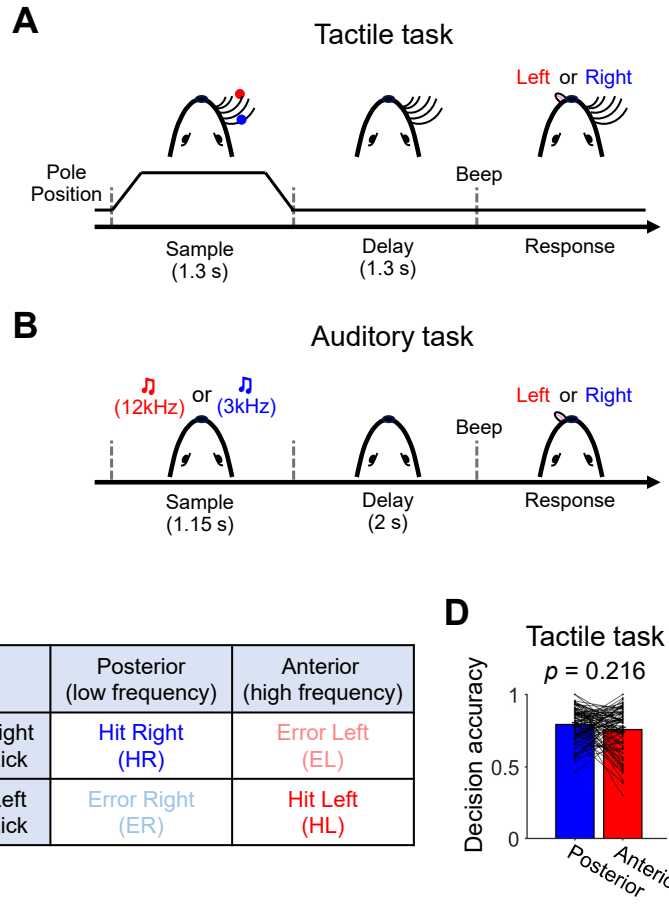

	Posterior (low frequency)	Anterior (high frequency)
Right Lick	Hit Right (HR)	Error Left (EL)
Left Lick	Error Right (ER)	Hit Left (HL)

Fig. 1. Task schematic for the delayed-response task and behavioral outcomes (A) Task schematic of the tactile delayed-response task. A pole was touched to an anterior or a posterior part of the whisker for 1.3 s (sample period), followed by a delay period of 1.3 s. In the response period, the mice licked to the left if the pole touched an anterior part of the whisker. Conversely, if the pole touched a posterior part of the whisker, mice licked to the right. (B) In the auditory delayed-response task, instead of tactile stimuli, auditory stimuli were presented. During a 1.15 s sample period, a 12 kHz or 3 kHz sound was presented, guiding the mice to lick to the left in case of a high frequency or lick to the right in case of a low frequency. After a delay of 2 s, the response period was initiated. (C) Possible behavioral outcomes in the perceptual delayed-response task depending on the match between the sensory stimulus (anterior vs. posterior in the tactile delayed-response task; low vs. high frequency in the auditory delayed-response task) and licking direction (left vs. right). Hit Right (HR): mice correctly licked to right in response to the posterior cue (or low frequency). Hit Left (HL): mice correctly licked to left in response to the anterior cue (or high frequency). Error Right (ER): mice incorrectly licked to left in response to the posterior cue (or low frequency). Error Left (EL): mice incorrectly licked to right in response to the anterior cue (or high frequency). (D) Decision accuracy in the tactile and auditory delayed-response tasks. Each line indicates the decision accuracy of a session. There was no significant difference in decision accuracy between the posterior and anterior cues (or low vs. high frequency) (two-sided Wilcoxon rank sum test, $p>0.1$).

aged firing rate vector, $\|v\|=\sqrt{\sum_{i=1}^{n} v_i^2}$. Here, v_i is the firing rate at the i-th time bin from the start of the baseline to the end of the delay period and n denotes the total number of time bins with the bin width of 50 ms (49-ms overlap). In our analysis, n=3150 in the tactile task and n=4274 in the auditory task. We divided the firing rates of single trials by the calculated norm. This baseline correction aligns with the baseline correction methods used in Yang's study [10] because it is particularly effective for normalizing neural activity when firing rates were concatenated across sessions. This preprocessing step was performed to remove baseline activity levels and ensure that the neural responses were scaled appropriately for comparison in further analyses.

Classification of selective neurons

ALM neurons exhibit selective activity in response to a specific stimulus or licking direction. This selectivity is an essential characteristic of ALM neurons when performing delayed-response task [6, 9]. To investigate how selectivity changed between the hit and error trials, selective neurons that exhibited significant firing rate differences between HR and HL were identified. In addition, to classify neurons as selective for a specific stimulus, the firing rate of a neuron over the bins within the sample period were averaged

and concatenated over the trials. Next, the average firing rates between the HR and HL trials were compared. Neurons that showed a significant difference in the average firing rate were classified as selective neurons (one-sided Wilcoxon rank-sum test, $p<0.01$). The stimulus to which selective neurons elicited higher firing rates was referred to as the preferred stimulus, whereas the stimulus associated with lower firing rates was referred to as the non-preferred stimulus. Similarly, an average firing rate was calculated across the delay period and selective neurons in the delay period were identified. The lick direction in which selective neurons showed a higher firing rate was referred to as the preferred lick direction, whereas the lick direction associated with lower firing rates was considered the non-preferred lick direction.

Inferring task-relevant signals from population activities

To investigate how stimulus and choice information are processed by ALM neurons during a delayed-response task, it is necessary to extract task-relevant ALM responses representing stimuli and choices. Thus, *sensory* (or *choice*) signals from the observed ALM activity were inferred by projecting population activity onto a low-dimensional space that maximally discriminated between stimuli (or choices). Specifically, we first averaged the normalized firing rate of ALM neurons across trials in each session. Average firing rates were then concatenated across sessions for all mice. This concatenation of neural data across different mice was supported by a study by Yang et al., who demonstrated that ALM neurons exhibit consistent neural response profiles across different mice [10]. The resulting firing rate matrix was of size N×T, where N is the number of neurons aggregated from all sessions and T is the number of time points used for the following inference (T=50). Using this firing-rate matrix, a sensory mode (SM) was inferred, defined as a linear projection vector that linked the N-dimensional population firing rates to a one-dimensional (1-D) space. In this 1-D space, the neural responses to different stimuli were maximally separated (posterior vs. anterior in the tactile delayed-response task and low vs. high frequency in the auditory delayed-response task). SM was inferred based on linear discrimination analysis (LDA) from the firing rates in each time bin in the sample period. However, the neural encoding of the stimulus could be incorrect in error trials. For example, in the error trials, the posterior tactile stimulus could be encoded incorrectly as if the anterior stimulus was given, or the stimulus could be encoded correctly, but with less distinctiveness compared to the hit trials. Consequently, to avoid such ambiguity in stimulus information encoded in neural activity during error trials, the error trials were excluded to infer a more reliable SM. After Step 2, the SM vectors were averaged across time bins in the sample period. Finally, the average SM was normalized to a unit length by dividing it by its norm.

The choice mode (CM) was defined as a linear projection vector that maximally separated neural responses to lick directions in a 1-D space (lick right vs. lick left). Similar to the SM, an N×T firing rate matrix was constructed; however, the delay period was considered instead of the sample period. Neural responses exhibit similar patterns when the same choice is made, irrespective of the correctness of the behavioral outcome [6]. Thus, in contrast to SM, error trials were used when inferring the CM. It was observed that the mice licked to the left even though the stimulus guided them to lick the right in the ER trials and licked to the right despite the stimulus guiding them to lick the left in the EL trials (Fig. 1C). When constructing the data matrix, the neural responses of the HR and EL and HL and ER were concatenated. After inferring the CM at each time bin in the delay period, the vectors of the CM were averaged across time bins in the delay period. Then, the averaged CM was normalized to have a unit length by dividing the CM by its norm as equation 1.

$$\vec{p}_{normalized} = \frac{\vec{p}}{\|\vec{p}\|} \quad (1)$$

The SM and CM were kept orthogonal to each other to prevent them from capturing overlapping information. This orthogonalization step enhanced the interpretability and specificity of the extracted signals. Finally, the sensory and choice signals were attained by projecting population activity via the SM and CM, respectively. As error trials were required to infer the CM, sessions in which both ER and EL trials occurred fewer than six times were excluded.

Decoding analysis

To evaluate the evolution of neural representations of sensory and choice information during the task, a support vector machine (SVM) classifier was built to predict a given stimulus or choice at each instant over the entire task period. Sessions in which either the number of HR or HL trials was less than 50 were excluded to ensure a sufficient number of trials for reliable decoding analysis. First, sensory signals were used to predict a given stimulus. To this end, 50 trials from each HR and HL trial were randomly sampled and 75% of them were used to infer SM (total 74 trials). Specifically, each HR and HL firing rate was averaged across trials and used to infer SM, as described above. The inferred SM was used to extract sensory signals for prediction. Using the same HR and HL trials (74 trials), a training set (x) was constructed to build the SVM. Specifically, x consisted of 1-D sensory signals at a given time instant averaged over a 30-ms window to reduce noise. Thus, the length of x was 37°C where 37 is the number of sampled tri-

https://doi.org/10.5607/en23020

als and C is the number of conditions (e.g., posterior vs. anterior or high vs. low frequency). A separate dataset was established to test the classifier performance. This test dataset was generated by randomly selecting 13 trials that were excluded from the training dataset. The firing rates were then concatenated from these selected trials across sessions. Firing rates were projected using the SM inferred from the training dataset. Finally, using the trained SVM classifier, the given stimulus was predicted based on the averaged sensory signals over a 30-ms window at every time instant during the task. This classification process was repeated 100 times from random sampling to the classification test. To determine the chance level of the SVM classifier, a permutation test was performed by randomly shuffling the assigned labels (given stimulus) for each feature vector. The SVM classifier was then applied to predict the labels and compute the average classification accuracy. This process was repeated 100 times to obtain an estimation of chance.

In addition, 37 of the hit trials were randomly sampled to infer CM. However, the number of erroneous trials could be less than 50. Nevertheless, data sets were augmented by randomly sampling the trials and concatenating the firing rate matrices across sessions. The CM was then inferred using a firing-rate matrix averaged across the sampled hit trials. After inferring CM, another classifier was built using a choice signal to predict the resulting lick direction. A feature vector x was constructed that consisted of choice signals averaged over a 30-ms window in the delay period. The length of x was 37*C where 37 is the number of sampled trials and C is the number of conditions (e.g., right lick vs. left lick). Note that we did not include the error trials when training the classifier. This is to test if choice signals during the error trials are built in a similar way to those in the hit trials. The performance of the classifier was tested by randomly sampling 13 test trials that were excluded from the training dataset. This classification process was repeated 100 times from random sampling to the classification test. To evaluate the chance level of the SVM classifier, a permutation test was conducted by randomly shuffling the labels (lick direction) associated with each feature vector. The SVM classifier was then used to predict labels based on the shuffled feature vectors, and the average classification accuracy was calculated. This process was performed 100 times to yield an estimation of chance performance.

RESULTS

Neural activities of selective neurons change in the error trials

Different groups of mice participated in one of the two perceptual delayed-response tasks (Fig. 1A, B). In the tactile delayed-response task, one group of mice was trained to discriminate the pole position. The pole was gently placed on either the anterior or the posterior whisker for 1.3 s (sample period, Fig. 1A). The mice received a non-selective auditory cue after 1.3 s of a temporal delay (delay period, Fig. 1A). Based on the tactile stimulus, the mice responded by licking either the right or left side to earn a water reward (response period, Fig. 1A). A separate group of mice was trained to perform the auditory delayed-response task. During the auditory delayed-response task, mice discriminated between auditory stimuli presented at two frequencies, 12 kHz (high frequency) or 3 kHz (low frequency). The auditory stimulus was presented for 1.15 s (sample period, Fig. 1B), followed by a 2 s delay (delay period, Fig. 1B). After a non-selective auditory cue, the mice licked to the left or right to receive a water reward (response period; Fig. 1B).

There were four possible behavioral outcomes depending on the match between the sensory stimulus (anterior vs. posterior in the tactile delayed-response task; low vs. high frequency in the auditory delayed-response task) and licking direction (left vs. right) (Fig. 1C). A trial was categorized as a hit right trial (HR) when the mice licked correctly to the right in response to a posterior cue (or low-frequency sound). Conversely, if the mice licked to the left when a posterior cue (or low-frequency sound) was given, it was recorded as an error-right trial (ER). When the mice licked correctly to the left in response to the anterior cue (or high-frequency sound), the trial was labeled a hit left trial (HL). Finally, if the mice incorrectly licked to the right in response to the anterior cue (or high-frequency sound), the trial was referred to as the error left trial (EL).

On average, in the tactile delayed-response task, each mouse performed 5.00±1.67 sessions over multiple days, where each session consisted of 65.37±26.53 HR, 17.29±12.47 ER, 63.60±25.93 HL, and 20.74±15.77 EL trials (MEAN±STD). Mice erroneously licked the left side in ER trials when a right-directional sensory cue was given, and the right side in EL trials when a left-directional sensory cue was given. The average ratio of the number of the error trials to the total number of trials was 23.25±9.72% (MEAN±STD). In the auditory delayed-response task, each mouse performed 3.33±1.32 sessions over multiple days, with each session consisting of 125.05±30.10 HR, 16.45±11.16 ER, 117.45±27.21 HL and 18.05±11.88 EL trials on average. The average ratio of the number of the error trials to the total number of trials was 12.89±8.41% (MEAN±STD).

We found no difference in decision accuracy between the HR and HL groups in both the tactile and auditory delayed-response tasks (Fig. 1D, two-sided Wilcoxon rank-sum test, $p>0.1$; n=95 sessions for the tactile delayed-response task; n=20 sessions for the auditory delayed-response task).

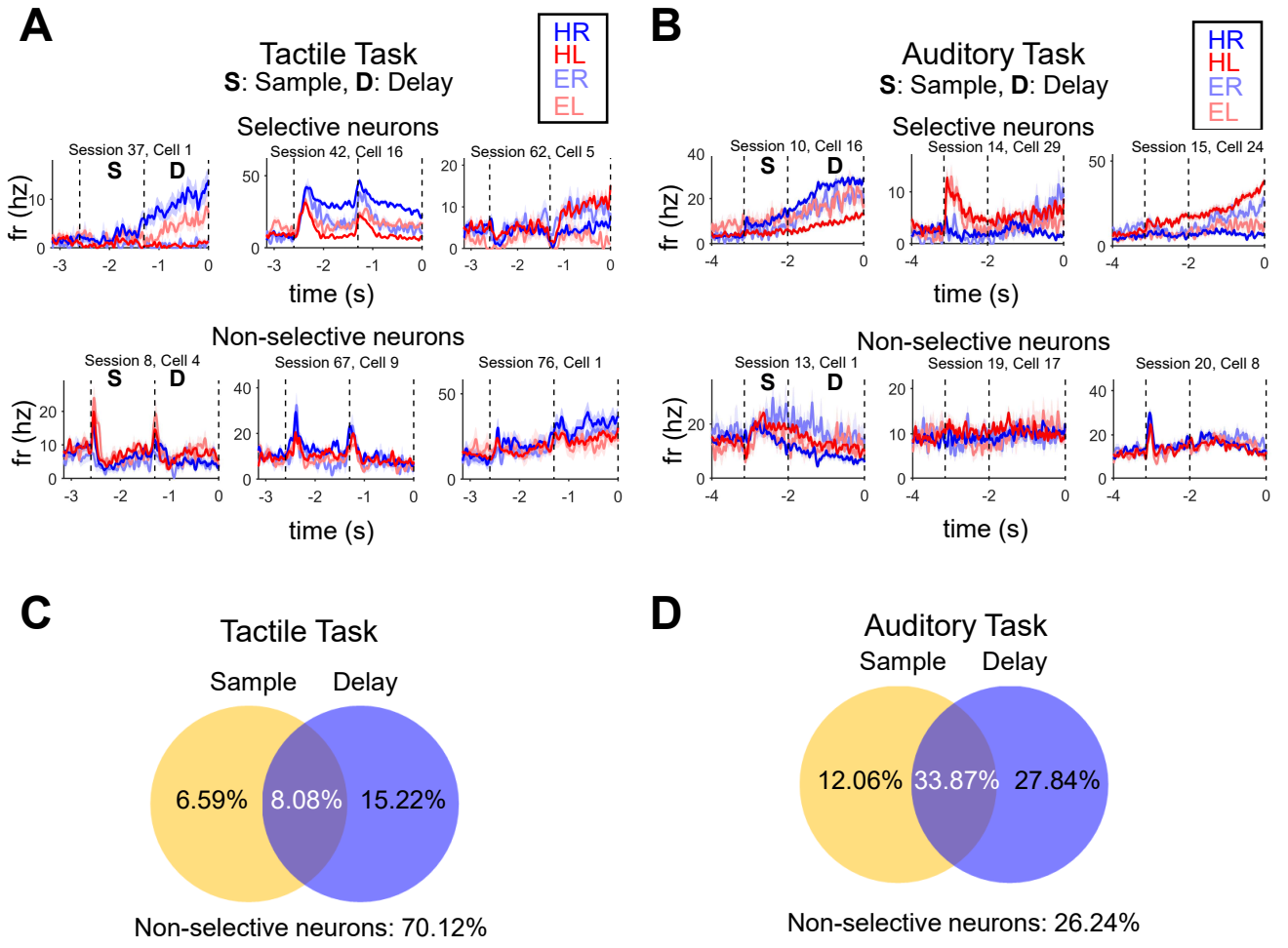

Fig. 2. Examples of firing rates of selective and non-selective neurons in (A) tactile delayed-response task (Top: selective neurons, bottom: non-selective neurons) and (B) auditory delayed-response task (Top: selective neurons, bottom: non-selective neurons). (A, B) S: Sample period, D: Delay period. Shaded regions indicate 95% confidence bounds. Firing rates are indicated by a blue solid line for the HR trials and a red solid line for the HL trials. (C) Percentages of selective and non-selective neurons during the tactile delayed-response task. (D) Percentages of selective and non-selective neurons during the auditory delayed-response task.

We observed that ALM neurons selectively increased their activity in response to specific stimuli or lick directions. For example, a neuron exhibited significantly higher activity during the delay period of the HR and EL trials when the animal licked to the right (Fig. 2A, Session 37, Cell 1). Similarly, another neuron showed increased activity in response to high-frequency auditory stimulus during the sample period (Fig. 2B, Session 14, Cell 29). We classified neurons as "selective" if they showed significantly higher activity in response to specific stimuli during the sample period or choice options during the delay period ($p<0.01$, one-sided Wilcoxon test) (Methods). Meanwhile, some neurons did not show selective activity during either the sample or delay period. These neurons were referred to as non-selective neurons (Fig. 2A, B bottoms). We encapsulated the proportions of selective and non-selective neurons across the task periods in Fig. 2C, D. ALM neurons showed diverse selective activities. Not all selective neurons during the sample period maintained their selectivity throughout the delay period (Fig. 2C, D, an intersecting area between the sample and delay). Furthermore, a larger number of neurons displayed selective activity, starting from the delay period.

We investigated whether the firing activity of selective neurons was maintained or changed during error trials. Selective neurons displayed significantly higher firing rates in response to the preferred stimulus (or preferred lick direction) than to the non-preferred stimulus (or non-preferred lick direction) (see every black dot below the unity line in Fig. 3A, B). However, in the error trials, we noticed that some neurons showed increased firing rates in response to the non-preferred stimulus (or non-preferred lick

https://doi.org/10.5607/en23020

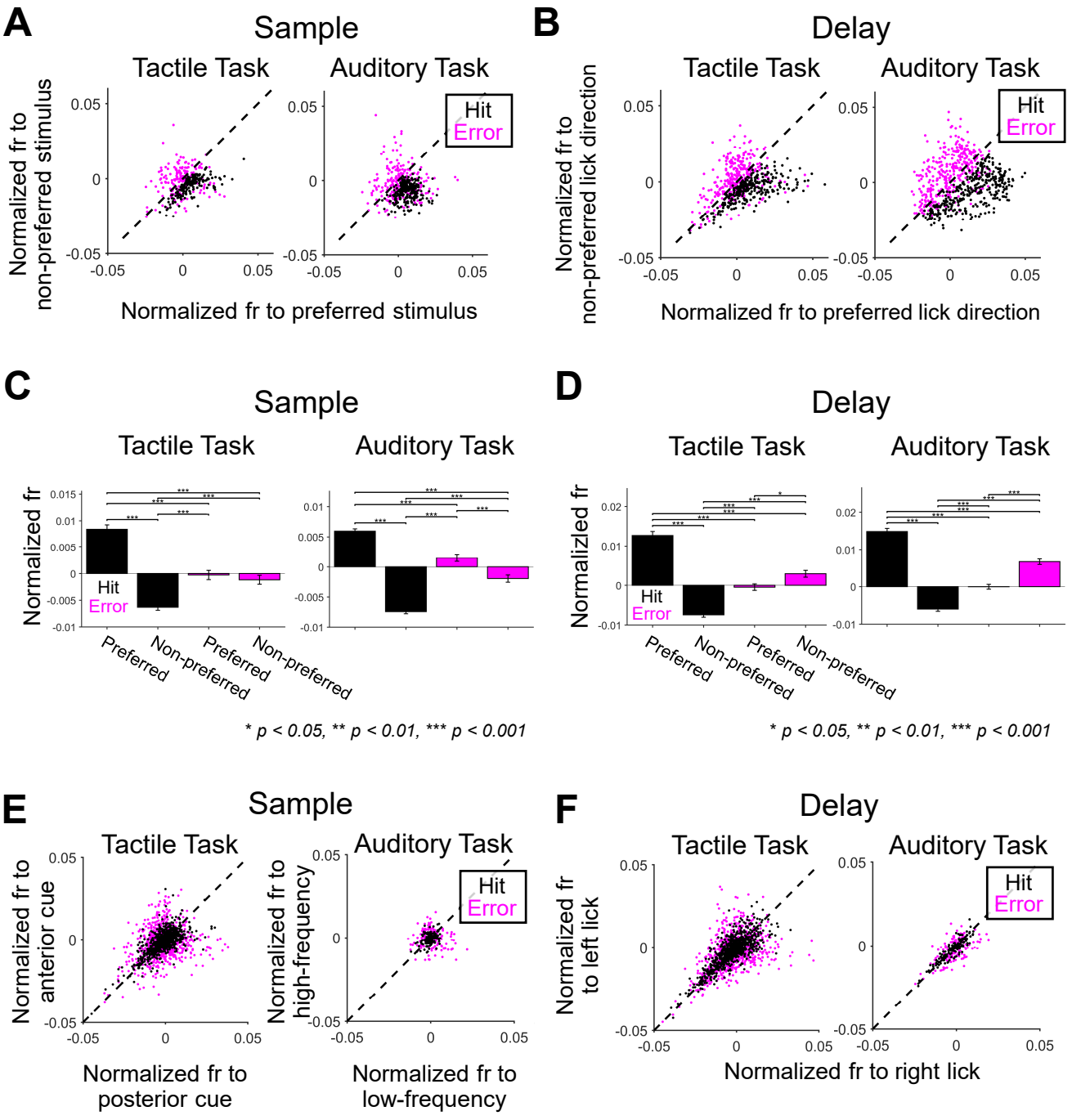

Fig. 3. Differences of neuronal selective activities to specific stimulus or lick direction between the hit and the error trials (A) Normalized firing rates (fr) to preferred and non-preferred stimuli during the sample period. (B) Normalized fr to preferred and non-preferred lick directions during the delay period. (A, B) Each dot indicates the normalized fr of a selective neuron in the hit (black) or error (pink) trial. The dotted line represents the unity line. (C) Changes in the normalized fr of selective neurons during the sample period (Bonferroni post hoc test). In the hit trials (black bars), the firing rates were significantly higher in response to the preferred stimulus than those to the non-referred stimulus (Bonferroni post hoc test, $p<0.001$). In the error trials (pink bars), the firing rates for the preferred stimulus were significantly lower than those in the hit trials (Bonferroni post hoc test, $p<0.001$). In addition, the firing rates for the non-preferred stimulus were significantly increased than those in the hit trials (Bonferroni post hoc test, $p<0.001$). (D) Changes in normalized fr of selective neurons during the delay period (Bonferroni post hoc test). In the hit trials, the firing rates of selective neurons were significantly higher when mice licked to the preferred direction compared to when mice licked to the non-preferred direction (Bonferroni post hoc test, $p<0.001$). On the contrary, in the error trials, the firing rates when mice licked to the non-preferred direction were significantly higher than those when mice licked to the preferred direction (Bonferroni post hoc test, $p<0.001$). (E) Normalized fr to the given stimulus during the sample period. (F) Normalized fr to the movement option (right- vs. left-) during the delay period. (E, F) Each dot indicates the normalized fr of a non-selective neuron in the hit (black) or error (pink) trial. The dotted line represents the unity line.

direction) (see pink-colored dots above the unity line in Fig. 3A, B). To measure the number of selective neurons that showed shifted activity during the error trials, we calculated the proportion of dots located above the unity line.

Among all selective neurons in the tactile delayed-response task (auditory delayed-response task), we observed that 48.4% (39.0%) of them showed lower firing rates for the preferred stimulus than for the non-preferred stimulus during the error trials (Fig. 3A). Similarly, among all selective neurons in the tactile delayed-response task (auditory delayed-response task), 57.3% (70.4%) of them showed lower firing rates for the preferred lick direction than for the non-preferred lick direction during the error trials (Fig. 3B).

Selective neurons showed significantly higher firing rates in response to the preferred stimulus (or lick direction) in hit trials (Fig. 3C, D). However, in the error trials, the overall firing rates of the selective neurons decreased (Fig. 3C, D). Specifically, in the sample period of the tactile delayed-response task, the firing rates for the preferred stimulus were not significantly different from those for the non-preferred stimulus (Bonferroni post hoc test, $p>0.05$) (Fig. 3C, left). During the sample period of the auditory delayed-response task, the firing rates for the non-preferred stimulus were lower than those for the preferred stimulus (Fig. 3C, right). However, during the delay period in both tasks, the firing rates for the non-preferred lick direction were higher than those for the preferred lick direction (Fig. 3D).

We conducted an additional analysis on non-selective neurons to investigate their firing activity in the hit and error trials. To this end, we calculated the firing rates of non-selective neurons in the HR trials and compared these to the firing rates in the HL trials. The same comparison was also made between the ER and EL trials. In the hit trials, non-selective neurons did not display any selective activities (as represented by the black dots centered around the unity line in Fig. 3E, F). However, in the error trials, some non-selective neurons showed selective firing activity (as represented by some of the pink dots that were deviated from the unity line in Fig. 3E, F). Yet, statistical evaluation of the firing rate differences between lick directions for non-selective neurons in the error trials revealed that only a minor fraction of non-selective neurons exhibited significant selective activity in the error trials for both tasks (ER vs. EL; $p<0.01$, a one-sided Wilcoxon test). In the tactile task, 6.15% of non-selective neurons showed selective activity during the sample period, and 6.60% during the delay period. Similarly, in the auditory task, 6.76% and 8.78% of non-selective neurons exhibited selective activity during the sample and delay periods, respectively.

In summary, selective neurons exhibited less salient selectivity and sometimes even increased activity for the non-preferred stimulus (or lick direction) during error trials compared with hit trials. However, because not all selective neurons showed reversed selectivity, it remained ambiguous whether changes in the firing activities of a subset of selective neurons caused erroneous decisions or if there were different neural substrates underlying erroneous decisions. In addition, a few non-selective neurons showed selective activity during error trials. Thus, we conducted further analyses to extract task-relevant signals from population activity.

Population activities encode sensory and choice information

We extracted task-relevant signals from ALM activity by projecting population activity onto a low-dimensional space that maximally discriminated between stimuli or choices (see Methods). To achieve this, we constructed firing rate matrices by averaging the normalized firing rates across trials (Fig. 4A, Step 1) and concatenating them across sessions, resulting in an N×T matrix (N: total neurons from all sessions, T: number of time points) (Fig. 4A, Step 1). Note that we used both selective and non-selective neurons in the following analyses. We used Linear Discriminant Analysis (LDA) to define the two key modes. The Sensory Mode (SM) is defined as a projection vector that maximizes the separation of neural responses to different stimuli during the sample period. In contrast, the Choice Mode (CM) is defined as a projection vector that differentiates between neural responses corresponding to different lick directions (i.e., lick right vs. lick left) during the delay period (Fig. 4A, Step 2). The SM and CM vectors were then averaged across the time bins and normalized (Fig. 4A, Step 3). To prevent overlapping information, SM and CM were orthogonal to each other. This step enhances the interpretability and specificity of the extracted signals (Fig. 4A, Step 4). Sensory and choice signals were obtained by projecting population activity through the SM and CM, respectively. If ALM neurons exhibit similar activity patterns to encode sensory and choice information, the SM and CM would be similar. However, we observed a clear discrepancy in the similarity values measured by the dot products between the SM and CM before orthonormalization (Fig. 4B, C). Because SM and CM were projection vectors to a low-dimensional space representing task-relevant variables (i.e., sensory and choice signals), the low similarity between these two vectors indicated that the weight of each neuron in the low-dimensional space differed. In other words, the engagement of each neuron in a population encoding sensory or choice information was different. This result is consistent with that of a previous study demonstrating that distinct groups of ALM neurons encode sensory or choice information in a perceptual delayed-response task [10].

https://doi.org/10.5607/en23020

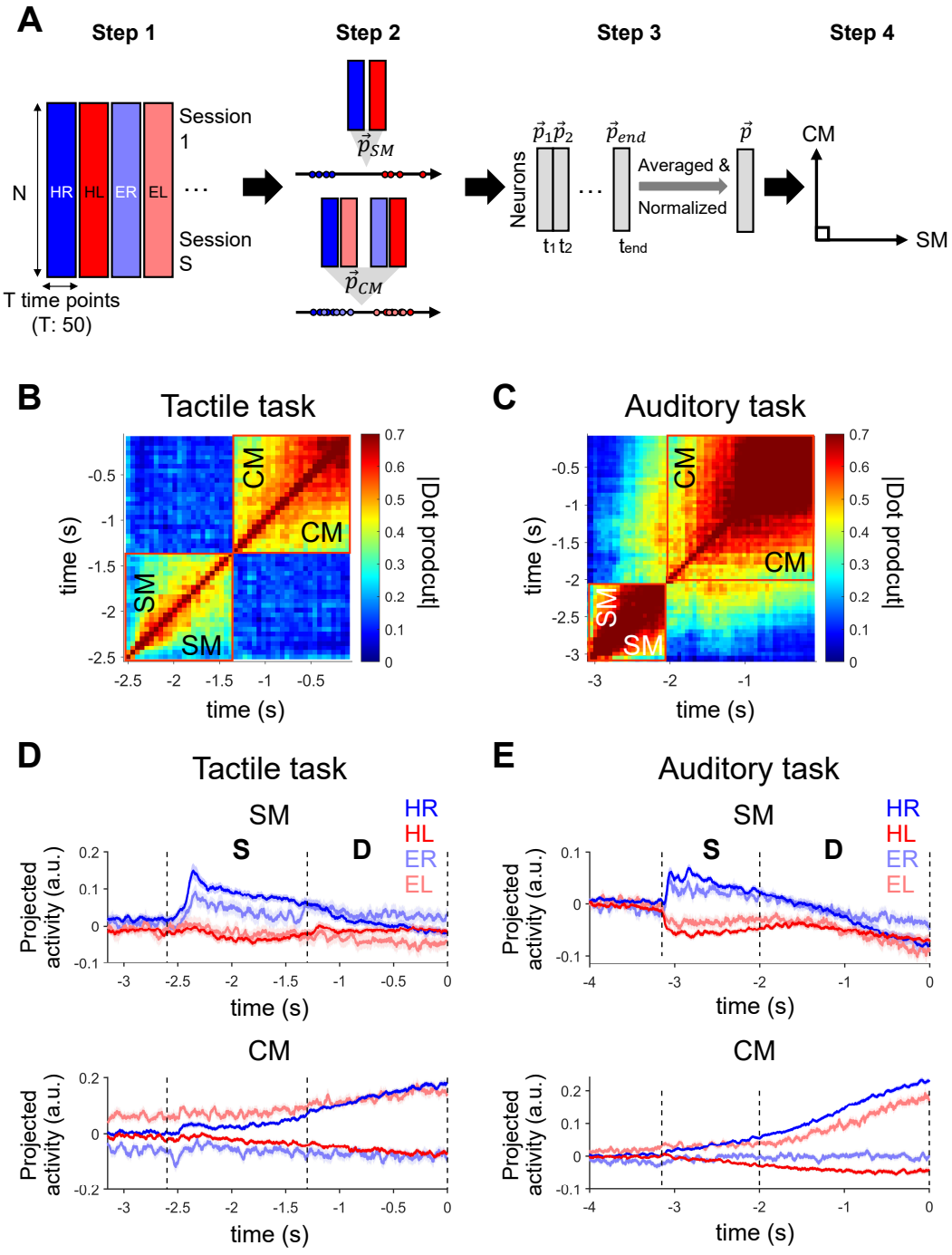

Fig. 4. ALM neurons show comprehensive activities of sensory and choice information. (A) Steps for inferring Sensory Mode (SM) and Choice Mode (CM). Step 1: A firing rate matrix was constructed every 50 ms. Note that we concatenated the firing rates across sessions (Methods). Step 2: A projection vector was inferred that discriminates sensory or choice information maximally. In inferring SM, we excluded the error trials. Step 3: Linear discriminant vectors were inferred over the sample period (or delay period) and averaged across time within the period. To infer SM (or CM), we used the firing rates during the sample period (or delay period). Step 4: SM and CM were kept orthonormal to each other for the specificity of the extracted signals. (B) Absolute dot products between SM and CM across time in the tactile delayed-response task. SM and CM were inferred at each time point before orthonormalization between them [steps 1~3 in (A)]. The sample and delay periods are marked by red boxes. (C) SM and CM in the auditory delayed-response task, as described in (B). (D) Sensory and choice signals obtained by projecting population activities onto one-dimensional spaces via SM (top) and CM (bottom) during the tactile delayed-response task. A solid line indicates mean sensory (bottom) or choice (top) signals across repetitions of calculating SM and CM. Shaded regions represent the standard deviation. Sensory signals exhibited similar temporal patterns between HR and ER or between HL and EL (top). Choice signals exhibited similar temporal patterns between HR and EL or between HL and ER (bottom). (E) Sensory and choice signals in the auditory delayed-response task, as described in (D).

In both tasks, we observed a transient increase in the absolute values of the sensory signals following the onset of the sample period. If the erroneous decision was made because sensory information was not encoded, then ALM neurons would not exhibit sensory signals to differentiate stimulus type. Alternatively, ALM neurons might encode stimulus information in a reversed fashion, potentially leading to erroneous decision-making. For example, when the left-guiding stimulus was given in the error trials, the sensory signals might display a similar activity pattern as those generated when the right-guiding stimulus was presented in the hit trials. However, sensory signals displayed comparable trajectories in both hit and error trials for the right-guiding stimulus (HR and ER in Fig. 4D top, Fig. 4E top), and similarly for the left-guiding stimulus (HL and EL in Fig. 4D top, Fig. 4E top).

To statistically confirm these observations, we employed statistical analysis to assess how distinguishable sensory signals were between right- and left-guiding stimuli. Using averaged sensory signals from multiple iterations, we examined the distinctiveness of these signals between stimuli. Specifically, we defined dH to represent the difference in sensory signals between HR and HL trials, and dE to represent the difference in sensory signals between ER and EL trials. As a result, both the length of dH and dE corresponded to the time points within the sample period.

Initially, to determine whether sensory signals differed between left- and right-guiding stimuli, we conducted a one-tailed paired t-test comparing dH (or dE) against 0. If the stimulus information was not encoded by ALM neurons, then differences between the sensory signals (dH and dE) would be close to 0. Or if ALM neurons encoded the stimulus type in a reversed manner in the error trials, then dE would be significantly less than 0 while dH is significantly greater than 0. We found that both dH and dE were significantly greater than 0 ($p<0.001$ for both tasks). Thus, the stimulus type was distinctly encoded in both hit and error trials, and the stimulus type (right- vs. left-guiding) was not reversely encoded in the error trials.

Next, we tested if the distinction between sensory signals for the right- and left-guiding stimuli in the error trials was less pronounced compared to the hit trials (Fig. 4D top, Fig. 4E top). We explored whether the sensory signals from the hit trials displayed a stronger directional selectivity compared to those from the error trials. For this purpose, we performed a one-tailed paired t-test between dH and dE. Our analysis confirmed that dH was significantly larger than dE ($p<0.001$). Together, the sensory signals effectively discriminated between the right- and left-guiding stimuli in both hit and error trials, although there was comparatively less distinctiveness in the error trials.

In the tactile delayed-response task, there was a time lag between the onset of the sample period and the increase in sensory signals (Fig. 4D, top), presumably due to the temporal delay required for the pole to fully touch the whisker. No such delay was observed in the auditory delayed-response task (Fig. 4E, top). The distinction in sensory signals between stimuli was most pronounced in the sample period and gradually diminished during the delay period in both tasks (Fig. 4D, E, top).

The choice signals gradually increased over time in both tasks. In the error trials, the choice signals tended to increase in the direction opposite to the guided licking direction (Fig. 4D, E, bottom). For example, in ER trials, where mice were guided to lick right but licked left instead, choice signals increased in alignment with the direction of the increase in choice signals observed in HL trials. To statistically validate this observation, we defined dH as the difference in choice signals between HR and HL during the sample period. Similarly, dE represented the difference in choice signals between ER and EL during the sample period. If the choice signals in the error trials followed similar trajectories as those in the hit trials, then dE would be also significantly greater than 0. However, we found that dE was significantly less than 0 while dH was significantly greater than 0 (one-tailed paired t-test, $p<0.001$ for both tasks). We conducted the same analysis on the choice signals during the delay period. We found the same results – while dH was significantly greater than 0, dE was significantly less than 0 (one-tailed paired t-test, $p<0.001$ for both tasks). These results support that even if the sensory signals encapsulated the given stimulus information, the choice signals diverged to the opposite direction of the guided lick direction (Fig. 4D bottom, Fig. 4E bottom).

Interestingly, in the error trials, we observed an offset in the CM even before the trial started (Fig. 4D, E, bottom). Specifically, during the pre-stimulus period, the choice signal shifted toward the HR trajectory in the EL trials and the HL trajectory in the ER trials. However, we could not observe this offset in the pre-stimulus period in the hit trials.

Choice bias exists during the pre-sample period in the error trials

We further investigated whether the offset of choice signals during the pre-stimulus period was biased toward the resulting lick direction. If the choice signals encoded a lick direction opposite to the guided lick direction, then the prediction of the resultant lick direction would surpass the chance level (approximately 50%). Consequently, the resultant lick direction contradicts the stimulus information encapsulated in sensory signals, which suggests that the formation of choice signals occurred independently of the provided stimulus information in the error trials.

To test this, we employed an SVM classifier trained with sensory

https://doi.org/10.5607/en23020

or choice signals to predict the given stimulus or resultant lick direction (see the Methods section). For succinctness, we refer to the decoding accuracy when predicting a given stimulus using sensory signals as $Accuracy_{SM}$ and predicting the resulting lick direction using choice signals as $Accuracy_{CM}$.

During the pre-stimulus period of the hit trials, $Accuracy_{SM}$ and $Accuracy_{CM}$ for both tasks were close to chance (Fig. 5A~D). However, during the prestimulus period of the error trials, $Accuracy_{CM}$ was significantly higher than chance ($p<0.001$, Bonferroni post hoc test), whereas $Accuracy_{SM}$ was not higher than chance (Fig. 5A~D). In the auditory delayed-response task, $Accuracy_{SM}$ differed between the hit and error trials across the prestimulus and sample periods ($p<0.001$, Bonferroni post hoc test; Fig. 5C). In addition, $Accuracy_{CM}$ was significantly higher in the error trials than in the hit trials and chance level in both tasks ($p<0.001$, Bonferroni post hoc test; Figs. 5B, D).

Throughout the sample period, $Accuracy_{SM}$ during the error trials exceeded chance levels. This trend is similarly observed in Fig. 4D, E, where sensory signals encoded the given stimulus, not the alternative stimulus during the error trials. These findings further strengthen the hypothesis that ALM neurons are capable of encoding the given stimulus information during the error trials.

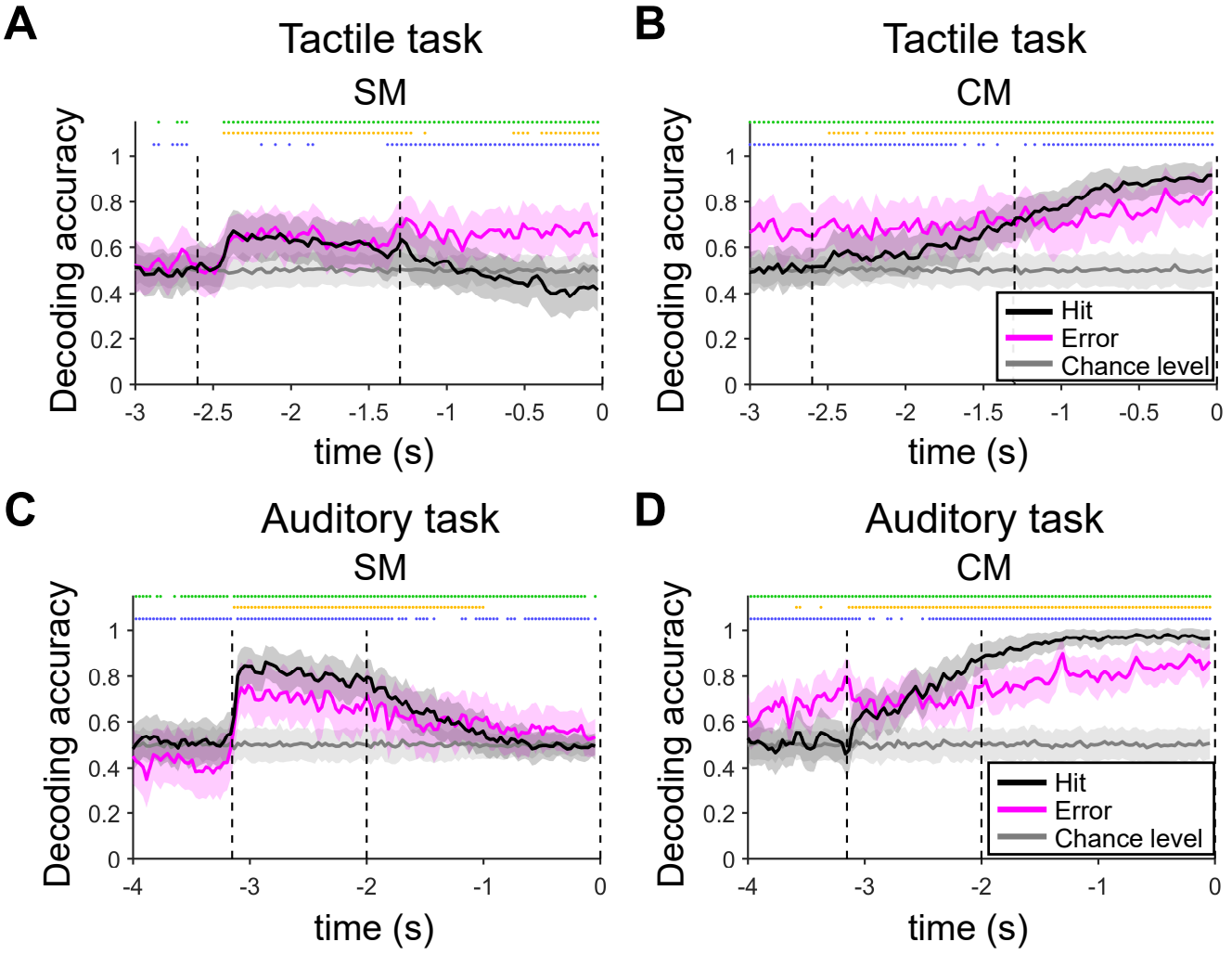

Fig. 5. Decoding performance to predict a given stimulus using sensory and or resulted choice using decoding signals. (A) Decoding performance of SVM classifier using sensory signals in the sample period (-2.6~-1.3 s) to predict the given stimulus across whole time points in the tactile delayed-response task. Shaded regions indicate standard deviation across iterations. Each dot indicates the time point where decoding accuracy is significantly different (purple dot: hit vs. the error trials, yellow dot: hit vs. chance level, green dot: error vs. chance level) (Bonferroni post hoc analysis, $p<0.001$). (B) Decoding performance of SVM classifier using choice signals in the delay period (-1.3~0 s) to predict the resulted lick direction across whole time points in the tactile delayed-response task. Shaded regions indicate standard deviation across iterations. Each dot indicates the time point where decoding accuracy is significantly different (purple dot: hit vs. the error trials, yellow dot: hit vs. chance level, green dot: error vs. chance level) (Bonferroni post hoc analysis, $p<0.001$). Similarly, (C) decoding accuracy of SVM classifier using sensory signals and (D) choice signals in the auditory delayed-response task.

However, $Accuracy_{SM}$ during the sample period in the error trials was lower than that during the hit trial, suggesting a weakened perception of the stimulus in the error trials (Fig. 5C). This reduced $Accuracy_{SM}$ was not observed in the tactile delayed-response task (Fig. 5A).

Nevertheless, $Accuracy_{CM}$ in the error trials was higher throughout the entire periods, including the presample, sample, and delay periods when predicting the resultant lick direction rather than the guided lick direction (Fig. 5B, D). This inference can be drawn from Fig. 4D, E, where the choice signals were biased towards the lick direction opposite the guided lick direction before the stimulus presentation.

In summary, these results tentatively suggest that sensory signals may still convey sensory information regarding a given stimulus, even in the error trials. However, choice signals became distinct between lick directions during the sample period.

DISCUSSION

In this study, we investigated why skillfully trained animals occasionally make erroneous decisions based on sensory information during choice tasks. We explored two potential factors of ALM activity that may contribute to erroneous decisions. First, we tested whether sensory information was abnormally encoded in the ALM. Second, we tested whether the alternations in neural activity were associated with the decision-making process. To this end, we analyzed two separate datasets of ALM recordings during which the mice performed the tactile or auditory delayed-response tasks. We observed alternations in the selective activities of individual neurons during both the sample and delay periods (Fig. 2A~D). Additionally, we examined how the representation of task-relevant variables, such as stimulus or choice, would be altered between hit and error trials. In both tasks, our observations tentatively suggested that while sensory information may become less distinctive, ALM neurons potentially retains some degree of information during the error trials (Fig. 4D, E, 5A, C). In contrast, the choice signals evolved toward incorrect directions in the error trials. Notably, despite bias not being advantageous in either task, we observed a bias towards a specific choice in the prestimulus period only in error trials. Additionally, we found that this bias in choice was mostly caused by selective rather than non-selective neurons (not shown in the present study). Therefore, we concluded that the presence of a bias in ALM activity towards a specific choice may hinder the utilization of correct sensory information and contribute to erroneous decision-making.

A previous study has indicated that ongoing neural activity can influence stimulus detection [15] and behavioral performance. For example, perceptual expectations can introduce biases at the beginning of the decision-making process [16]. Neural oscillation studies have found that behavioral performance depends on the amplitude of oscillations during the prestimulus period [17-19]. In addition, sensory information presented in the late phase does not influence the decisions [2]. These findings suggest that if the ongoing neural activity preceding the stimulus presentation occasionally reaches a certain state, it may become difficult to reverse its dynamics using external information. In our study, once the decision-making process progressed to a certain stage before the trial began, it became less susceptible to the influence of sensory information in the opposite direction.

We analyzed two separate datasets involving different sensory modalities and observed common substrates underlying erroneous decisions. We observed an offset in the choice signals during the pre-sample period in the error trials, regardless of sensory modality. Simultaneously, we noticed minor differences between the tasks. In the tactile delayed-response task, there was no offset in the sensory signals during the pre-stimulus period (Fig. 5A). In addition, there was no significant difference in the decoding accuracy during the sample period between the hit and error trials. However, in the auditory delayed-response task, we observed an offset in the sensory signals in the direction opposite to that of the given stimulus (Fig. 5C). This discrepancy in accuracy persisted throughout the sample period (Fig. 5C). These differences may originate from the differences in sensory modalities (tactile vs. auditory). For instance, the suppression of the auditory cortex during the early phase of the delay period impairs working memory, suggesting its involvement in the maintenance of working memory [20]. However, a similar suppression of the vS1 in the delay period does not affect working memory [6, 21], suggesting that working memory may be differently influenced by sensory information processing in the two modalities. Hence, the differences in the sensory modalities observed in this study may reflect the utilization of sensory information in working memory tasks.

If an increment in choice signals over time is indicative of confidence, choice signals would decrease when conflicting evidence is presented (i.e., presentation of a stimulus opposite to biased choice signals in error trials). However, the choice signals gradually moved in the opposite direction, with no decreasing tendency in the error trials during the sample period (Fig. 5C, D). An alternative explanation for this increase in choice signals could be the effect of urgency signals on the decision-making process [2, 3]. This urgency signal originates from brain regions external to the ALM and drives timely decision-making while maintaining robustness against distracting sensory signals [2]. In this scenario, the urgency signal acts as a stabilizing force that reinforces the initial bias and

https://doi.org/10.5607/en23020

reduces the likelihood of changing decisions.

Multiple brain regions are reportedly involved with the ALM in the perceptual delayed-response task, including the sensory cortex, medial motor cortex, thalamus, and cerebellum [9, 21-24]. Future studies need to test whether the bias observed in this study is only present in the ALM or is shaped through computations across multiple regions. Also, further research is required to investigate how biases are shaped and how they affect the decision-making process over trials. They can also be related to memory consolidation during learning the task. Investigating changes in the sensory and control signals of ALM populations during learning will particularly be intriguing to understand the sources of biases. Biases can arise from various sources, including the outcomes of preceding trials or preferences for a specific click direction. Further, it is important to address whether there is indeed no bias in the hit trials or whether there exists a weak bias that may have been canceled out after the averaging processes. Large-scale neural recordings are effective for capturing heterogeneous neural dynamics and identifying sources of bias within individual subjects [25]. By examining neural activity patterns and their relationship with bias, we may gain deeper insight into the mechanisms underlying bias formation and its influence on sensorimotor transformation.

ACKNOWLEDGEMENTS

This study was supported by the Brain Convergence Research Programs of the National Research Foundation (NRF) funded by the Korean government (MSIT) (NRF 2019M3E5D2A01058328) and the Alchemist Project Brain to X (B2X) Project funded by the Ministry of Trade, Industry and Energy (No. 20012355; NTIS No. 1415181023).

REFERENCES

1. Hernández A, Nácher V, Luna R, Zainos A, Lemus L, Alvarez M, Vázquez Y, Camarillo L, Romo R (2010) Decoding a perceptual decision process across cortex. Neuron 66:300-314.
2. Finkelstein A, Fontolan L, Economo MN, Li N, Romani S, Svoboda K (2021) Attractor dynamics gate cortical information flow during decision-making. Nat Neurosci 24:843-850.
3. Inagaki HK, Chen S, Daie K, Finkelstein A, Fontolan L, Romani S, Svoboda K (2022) Neural algorithms and circuits for motor planning. Annu Rev Neurosci 45:249-271.
4. Inagaki HK, Fontolan L, Romani S, Svoboda K (2019) Discrete attractor dynamics underlies persistent activity in the frontal cortex. Nature 566:212-217.
5. Inagaki HK, Inagaki M, Romani S, Svoboda K (2018) Low-dimensional and monotonic preparatory activity in mouse anterior lateral motor cortex. J Neurosci 38:4163-4185.
6. Li N, Chen TW, Guo ZV, Gerfen CR, Svoboda K (2015) A motor cortex circuit for motor planning and movement. Nature 519:51-56.
7. Li N, Daie K, Svoboda K, Druckmann S (2016) Robust neuronal dynamics in premotor cortex during motor planning. Nature 532:459-464.
8. Wu Z, Litwin-Kumar A, Shamash P, Taylor A, Axel R, Shadlen MN (2020) Context-dependent decision making in a premotor circuit. Neuron 106:316-328.e6.
9. Guo ZV, Inagaki HK, Daie K, Druckmann S, Gerfen CR, Svoboda K (2017) Maintenance of persistent activity in a frontal thalamocortical loop. Nature 545:181-186.
10. Yang W, Tipparaju SL, Chen G, Li N (2022) Thalamus-driven functional populations in frontal cortex support decision-making. Nat Neurosci 25:1339-1352.
11. Ma WJ, Beck JM, Latham PE, Pouget A (2006) Bayesian inference with probabilistic population codes. Nat Neurosci 9:1432-1438.
12. Komiyama T, Sato TR, O'Connor DH, Zhang YX, Huber D, Hooks BM, Gabitto M, Svoboda K (2010) Learning-related fine-scale specificity imaged in motor cortex circuits of behaving mice. Nature 464:1182-1186.
13. Chae S, Sohn JW, Kim SP (2022) Investigation of neural substrates of erroneous behavior in a delayed-response task. eNeuro 9:ENEURO.0490-21.2022.
14. Li N, Gerfen CR, Svoboda K (2014) Extracellular recordings from anterior lateral motor cortex (ALM) neurons of adult mice performing a tactile decision behavior [Internet]. Plone Foundation. Available from: https://doi.org/10.6080/K0M-S3QNT.
15. Rassi E, Wutz A, Müller-Voggel N, Weisz N (2019) Prestimulus feedback connectivity biases the content of visual experiences. Proc Natl Acad Sci U S A 116:16056-16061.
16. de Lange FP, Rahnev DA, Donner TH, Lau H (2013) Prestimulus oscillatory activity over motor cortex reflects perceptual expectations. J Neurosci 33:1400-1410.
17. Linkenkaer-Hansen K, Nikulin VV, Palva S, Ilmoniemi RJ, Palva JM (2004) Prestimulus oscillations enhance psychophysical performance in humans. J Neurosci 24:10186-10190.
18. Kluger DS, Balestrieri E, Busch NA, Gross J (2021) Respiration aligns perception with neural excitability. Elife 10:e70907.
19. Iemi L, Gwilliams L, Samaha J, Auksztulewicz R, Cycowicz YM, King JR, Nikulin VV, Thesen T, Doyle W, Devinsky O, Schroeder CE, Melloni L, Haegens S (2022) Ongoing neural oscillations influence behavior and sensory representations

by suppressing neuronal excitability. Neuroimage 247:118746.
20. Yu L, Hu J, Shi C, Zhou L, Tian M, Zhang J, Xu J (2021) The causal role of auditory cortex in auditory working memory. Elife 10:e64457.
21. Guo ZV, Li N, Huber D, Ophir E, Gutnisky D, Ting JT, Feng G, Svoboda K (2014) Flow of cortical activity underlying a tactile decision in mice. Neuron 81:179-194.
22. Duan CA, Pagan M, Piet AT, Kopec CD, Akrami A, Riordan AJ, Erlich JC, Brody CD (2021) Collicular circuits for flexible sensorimotor routing. Nat Neurosci 24:1110-1120.
23. Gao Z, Davis C, Thomas AM, Economo MN, Abrego AM, Svoboda K, De Zeeuw CI, Li N (2018) A cortico-cerebellar loop for motor planning. Nature 563:113-116.
24. Wang Y, Yin X, Zhang Z, Li J, Zhao W, Guo ZV (2021) A cortico-basal ganglia-thalamo-cortical channel underlying short-term memory. Neuron 109:3486-3499.e7.
25. Steinmetz NA, Aydin C, Lebedeva A, Okun M, Pachitariu M, Bauza M, Beau M, Bhagat J, Böhm C, Broux M, Chen S, Colonell J, Gardner RJ, Karsh B, Kloosterman F, Kostadinov D, Mora-Lopez C, O'Callaghan J, Park J, Putzeys J, Sauerbrei B, van Daal RJJ, Vollan AZ, Wang S, Welkenhuysen M, Ye Z, Dudman JT, Dutta B, Hantman AW, Harris KD, Lee AK, Moser EI, O'Keefe J, Renart A, Svoboda K, Häusser M, Haesler S, Carandini M, Harris TD (2021) Neuropixels 2.0: a miniaturized high-density probe for stable, long-term brain recordings. Science 372:eabf4588.

 https://doi.org/10.5607/en23020